

A simple method to measure critical angles for high-sensitivity differential refractometry

S. C. Zilio

Instituto de Física de São Carlos, Universidade de São Paulo, CP 369, 13560-970 São Carlos, SP, Brazil
zilio@ifsc.usp.br

Abstract: A total internal reflection-based differential refractometer, capable of measuring the real and imaginary parts of the complex refractive index in real time, is presented. The device takes advantage of the phase difference acquired by *s*- and *p*-polarized light to generate an easily detectable minimum at the reflected profile. The method allows to sensitively measuring transparent and turbid liquid samples.

©2012 Optical Society of America

OCIS codes: (260.6970) Total internal reflection; (280.4788) Optical sensing and sensors; (290.7050) Turbid media; (230.0230) Optical devices.

References and links

1. G. H. Meeten and A. N. North, "Refractive index measurement of absorbing and turbid fluids by reflection near the critical angle," *Meas. Sci. Technol.* **6**(2), 214–221 (1995).
2. A. J. Jääskeläinen, K. E. Peiponen, and J. A. Rätty, "On reflectometric measurement of a refractive index of milk," *J. Dairy Sci.* **84**(1), 38–43 (2001).
3. W. R. Calhoun, H. Maeta, A. Combs, L. M. Bali, and S. Bali, "Measurement of the refractive index of highly turbid media," *Opt. Lett.* **35**(8), 1224–1226 (2010).
4. W. R. Calhoun, H. Maeta, S. Roy, L. M. Bali, and S. Bali, "Sensitive real-time measurement of the refractive index and attenuation coefficient of milk and milk-cream mixtures," *J. Dairy Sci.* **93**(8), 3497–3504 (2010).
5. M. McClimans, C. LaPlante, D. Bonner, and S. Bali, "Real-time differential refractometry without interferometry at a sensitivity level of 10^{-6} ," *Appl. Opt.* **45**(25), 6477–6486 (2006).
6. G. R. Fowles, *Introduction to Modern Optics*, Holt, Rinehart and Winston, Inc., New York, 1968.
7. M. H. Chiu, J. Y. Lee, and D. C. Su, "Complex refractive-index measurement based on Fresnel's equations and the uses of heterodyne interferometry," *Appl. Opt.* **38**(19), 4047–4052 (1999).
8. S. T. Flock, B. C. Wilson, and M. S. Patterson, "Total attenuation coefficients and scattering phase functions of tissues and phantom materials at 633 nm," *Med. Phys.* **14**(5), 835–841 (1987).
9. <http://refractiveindex.info>
10. S. C. Zilio, "Refratômetro diferencial para medir o índice de refração e coeficiente de atenuação de um líquido em tempo real", Patent pending.

1. Introduction

The measurement of critical angles (θ_c) in total internal reflection (TIR) has found increasing use in differential refractometry, particularly for absorbing or turbid samples [1–4]. In a recent work, McClimans *et al.* [5] demonstrated a technique for measuring the refractive index of transparent liquid samples at a sensitivity level of 10^{-6} by using a divergent laser beam, polarized parallel to the plane of incidence (*p*-polarization), and a linear diode array to precisely find the critical angle. The technique relies on measuring the intensity angular distribution of the divergent laser beam totally reflected by a high-index prism. Normalizing the profile obtained with a particular liquid sample to that obtained with air yields the Fresnel reflectance. At the vicinity of θ_c the reflection changes abruptly, and then, it is possible to find the critical angle with a good sensitivity. Since the absolute value of θ_c is not measured, the results have to be calibrated against a known sample, with an Abbe refractometer or similar, which turn this into a differential technique that needs an origin for refractive indices values.

For absorbing or turbid samples, the critical angle is not well defined and one relies in secondaries procedures, such as using the derivative of the reflectance profile [2], as done in many commercial devices, or fitting the reflected profile with a Fresnel theory modified to

include the effect of angle-dependent penetration into the turbid medium [3, 4]. One of the drawbacks of all method used up to date to find θ_c , for turbid or even transparent samples, is related to possible laser power fluctuations during the measurements. This occurs because the measurement is carried out in the TIR condition where the reflected light is intense. This problem would be avoided if the measurement was performed in a condition where the signal is at a minimum.

The present work takes advantage of the different phase changes acquired during the internal reflection by light polarized parallel (p) and perpendicular (s) to the plane of incidence, to generate a signal that has a minimum at θ_c . In the particular case where the medium is transparent, the value of the minimum is zero. As a consequence, one has a dark stripe on the reflected intensity pattern at the critical angle that makes its determination very easy. For turbid samples, the minimum does not reach zero, but even though is easily determined. This method promptly provides the values of the refractive index and extinction coefficient in real time, without any complicated fitting procedure.

2. Experimental section

The experimental arrangement, shown in Fig. 1, is similar to that employed in [5] but in order to avoid an optical fiber or additional lens to diverge the beam, it uses a semicylindrical lens, with a radius of 10 mm and height of 7 mm, made of flint glass (Schott, SF10), instead of an equilateral prism. Regardless of how well the incoming beam is collimated, the lens automatically gives simultaneous access to many different incident angles. The reflected profile is detected by an inexpensive CCD Web camera, and processed with the LabVIEW software that provides the light intensity reaching each pixel of the CCD and generates a profile for a specified horizontal line of the image. To improve the signal-to-noise ratio, the profiles of several horizontal adjacent lines close to the image's center are collected and averaged. As light source, a low-cost green laser pointer (532 nm) is normally used, but to better characterize the linearity of the optical system we also employed a tunable He-Ne laser. The light leaving the laser passes through a polarizer with transmission axis at 45° with the vertical such that the components parallel and perpendicular to the plane of incidence have equal amplitudes. An analyzer, with the transmission axis parallel to that of the input polarizer, is placed in front of the CCD camera. An acrylic holder allows the liquid sample to make contact with the lens base.

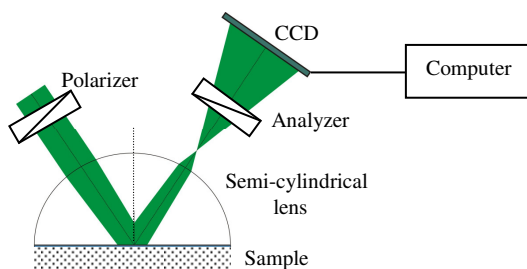


Fig. 1. Schematic view of the refractometer.

3. Origin of the dark stripe

To promptly understand the origin of the dark line at θ_c , we first consider a transparent medium and write the Fresnel reflection coefficients for s - and p -polarized light as [6]:

$$r_s = \frac{\cos \theta - \sqrt{n^2 - \sin^2 \theta}}{\cos \theta + \sqrt{n^2 - \sin^2 \theta}}, \quad (1)$$

$$r_p = \frac{-n^2 \cos \theta + \sqrt{n^2 - \sin^2 \theta}}{n^2 \cos \theta + \sqrt{n^2 - \sin^2 \theta}}, \quad (2)$$

where θ is the angle of incidence and $n = n_{\text{sample}}/n_{\text{glass}} < 1$ is the relative refractive index. Above the Brewster's angle, the p -component acquires a phase π and changes its signal, thus rotating the polarization by 2α , where $\tan \alpha = |r_s|/|r_p|$. Therefore, a fraction of the reflected light passes through the analyzer, as shown in the left part of Fig. 2(a). As the incident angle approaches θ_c , $|r_s|$ and $|r_p|$ tend to 1, but because the electric field of the p -polarized light gained a π phase change, the polarization of the reflected light is rotated by 90° . As consequence, the light is blocked by the analyzer. Above the critical angle, the amplitudes are always the same ($|r_s| = |r_p| = 1$), but there is a phase difference occurring during the total internal reflection, given by [6]:

$$\delta = \theta_\sigma - \theta_\pi = \pi - 2 \left\{ \tan^{-1} \left(\sqrt{\sin^2 \theta - n^2} / \cos \theta \right) - \tan^{-1} \left(\sqrt{\sin^2 \theta - n^2} / n^2 \cos \theta \right) \right\}, \quad (3)$$

such that the intensity transmitted through the analyzer is proportional to $(1 + \cos \delta)$. As consequence, the reflected light passes again through the analyzer, leaving a dark stripe at θ_c , as seen in the theoretical curve (a) of Fig. 2 and in the experimental pattern of Fig. 3(a).

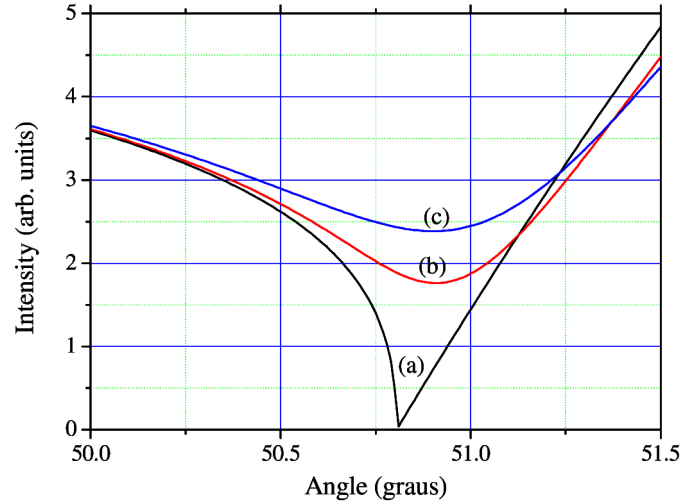


Fig. 2. Light transmitted through the analyzer as a function of incidence angle for (a) $\alpha = 0$ cm^{-1} , (b) $\alpha = 1000 \text{ cm}^{-1}$ and (c) $\alpha = 2000 \text{ cm}^{-1}$. We used $n = 0.775$ and $\alpha = (4\pi/\lambda)kn_{\text{glass}}$.

The situation is somewhat more involved if the medium is turbid or absorbing. In this case, the relative index of Eqs. (1) and (2) must be replaced by the complex relative index of refraction $\tilde{n} = n + ik$, where k is the attenuation coefficient of the sample, due to absorption and scattering, divided by the glass index. Following the analysis of [7], these equations become:

$$r_s = \frac{\cos \theta - \sqrt{\tilde{n}^2 - \sin^2 \theta}}{\cos \theta + \sqrt{\tilde{n}^2 - \sin^2 \theta}} = \frac{\cos \theta - (u + iv)}{\cos \theta + (u + iv)} = |r_s| \exp(i\delta_s), \quad (4)$$

$$r_p = \frac{-\tilde{n}^2 \cos \theta + \sqrt{\tilde{n}^2 - \sin^2 \theta}}{\tilde{n}^2 \cos \theta + \sqrt{\tilde{n}^2 - \sin^2 \theta}} = \frac{-\tilde{n}^2 \cos \theta + (u + iv)}{\tilde{n}^2 \cos \theta + (u + iv)} = |r_p| \exp(i\delta_p), \quad (5)$$

where

$$u^2 = \frac{1}{2} \left\{ (n^2 - k^2 - \sin^2 \theta) + \sqrt{(n^2 - k^2 - \sin^2 \theta)^2 + 4n^2 k^2} \right\}, \quad (6)$$

$$v^2 = \frac{1}{2} \left\{ -(n^2 - k^2 - \sin^2 \theta) + \sqrt{(n^2 - k^2 - \sin^2 \theta)^2 + 4n^2 k^2} \right\}. \quad (7)$$

As discussed in [3] and [4], the refraction in a turbid medium leads to an angle-dependent penetration that can be accounted for by substituting the constant k by $k(\theta) = k[4\pi\sqrt{(M-L)/2}]^{-1}$, where $L = n^2 - k^2 - \sin^2 \theta$ and $M^2 = P^2 - 2L \sin^2 \theta - \sin^4 \theta$, with $P^2 = n^2 + k^2$. After some algebra, the above set of equations provides the amplitudes and phase of the reflectivity coefficients. The intensity reaching the CCD is proportional to $|r_s|^2 + |r_p|^2 + 2|r_s||r_p|\cos(\delta_s - \delta_p)$ and is shown in Fig. 2 for two values of attenuation coefficients, defined as $\alpha = (4\pi/\lambda) k n_{\text{glass}}$. Therefore, by measuring the values of the minimum position and its amplitude one can find the complex refractive index. For practical purposes, we analyzed several curves like those of Fig. 2 and found that for $\alpha < 200 \text{ cm}^{-1}$, the minimum can be characterized approximately by:

$$\theta_{\min} \approx \sin^{-1} n, \quad (8)$$

$$V_{\min} \propto k. \quad (9)$$

Nevertheless, both θ_{\min} and V_{\min} have to be calibrated against some reference sample with known values of n and k . The calibration for n may be achieved by measuring two transparent solutions in a commercial refractometer and the calibration for k may be obtained by analyzing the transmission of a collimated beam through a thin cell containing some phantom material, according to the method described in [8].

4. Results and discussion

Figure 3 shows the image captured by the CCD webcam in the case where the sample is distilled water. Since in this example $\alpha = 0$, one can determine the critical angle in a condition of zero-signal, which completely avoids the problem of laser fluctuation. For transparent media, however, we are interested just in finding the location of the minimum, which does not depend on the laser power. Therefore, we can work with the CCD saturated, as shown in Fig. 3(b), and under this condition, θ_c can be found with a good sensitivity, even though the minimum value is not zero.

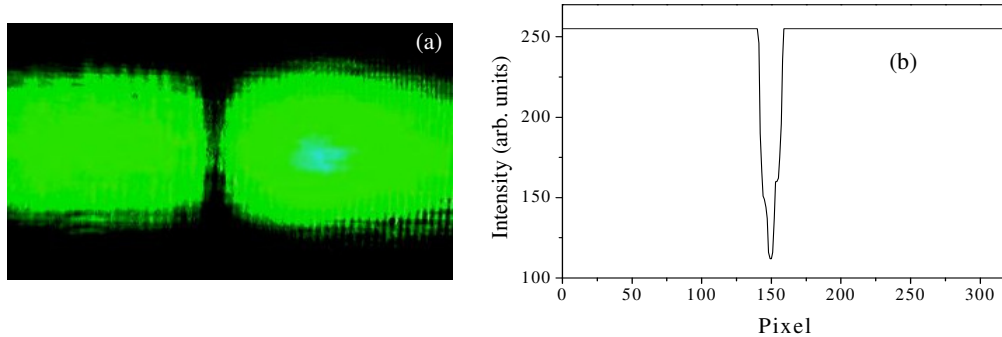


Fig. 3. (a) Image captured by the CCD webcam. (b) Intensity along the horizontal line at the center of the profile, for the saturated condition. In these figures, the sample in contact with the semi-cylindrical lens is water.

As in the method described in [5], the present technique is also of the differential type, meaning that it allows the measurement of small changes of refractive indices around a known (calibrated) value. Our first concern is to verify the dependence of the pixel position where the dark line is detected on the critical angle. This was accomplished with the tunable He-Ne laser using distilled water as sample. Since the refractive index of the SF10 and water are known [9], we can calculate $\theta_c (= \sin^{-1} n_{\text{water}}/n_{\text{SF10}})$ for the several spectral lines of the laser and plot it against the pixel position where the dark line appears. For a given wavelength λ_0 , the critical angle measured is denoted as $\theta_c(\lambda_0)$. For a nearby wavelength λ , the new angle is $\theta_c(\lambda) = \theta_c(\lambda_0) + \Delta\theta$, such that $n(\lambda) = \sin \theta_c(\lambda) \approx n(\lambda_0) + \cos \theta_c(\lambda_0) \Delta\theta$, for small $\Delta\theta$. Therefore, a linear behavior between n and $\Delta\theta$ is expected for sufficiently small variations of n . Indeed, such dependence was observed for the orange/red lines (594, 604, 612 and 633 nm) but the green line (543 nm) deviates somewhat from the linear behavior. Furthermore, the chromatic focal shift should also be considered in the case of large spectral variation. In this experiment $n_{\text{water}}/n_{\text{SF10}}$ changed by more than 10^{-3} , but in measurements where the relative indices change less than 10^{-4} , and the wavelength is fixed, the linear behavior can be safely assumed.

After validating the linearity between θ_c and the pixel number, we used this refractometer to demonstrate changes in the refractive index that are smaller than 10^{-5} . Solutions of different volume concentrations of ethanol ($n = 1.36371$ @ 532 nm, 20 °C) in water ($n = 1.33524$ @ 532 nm, 21.5 °C), ranging from 0 to 1%, were used. The values of refractive indices of ethanol, water and the SF10 glass were taken from [9]. For calibration, we used a commercial Pulfrich refractometer with a resolution better than 10^{-5} . The indices were measured at 546 nm (Hg, spectral line e) and then corrected to 532 nm. The temperature was kept constant in ± 0.2 °C around 22 °C. Figure 4 depicts the results obtained with the Pulfrich refractometer and with the proposed technique, proving that it is capable of providing sensitivity better than 10^{-5} . The refractive indices obtained with the Pulfrich refractometer can be used to calibrate the pixel number scale. Note that after a calibration, prior to carry out any further measurements of unknown samples, the position of the CCD relative to the lens cannot be changed.

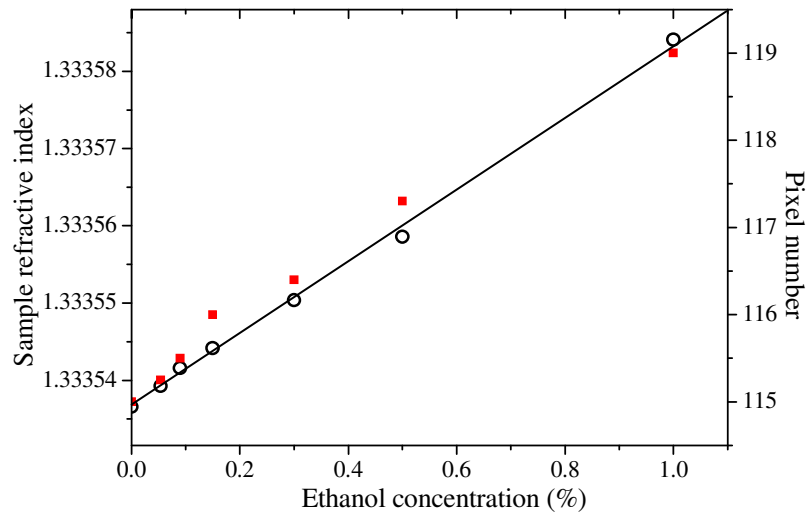


Fig. 4. Refractive index obtained with a Pulfrich refractometer (open circles) and position of the dark line measured with the present refractometer (red squares). The solid line is just a guide for the eye.

As another example of the usefulness of this refractometer, measurements were performed in different types of milk, which is known to be a medium with moderate turbidity ($\alpha < 200$

cm^{-1}) [4]. In this case, the CCD signal is not saturated in order to guarantee the linear behavior of V_{\min} . Three types of milk of the same brand were used, with nominal fat concentration of ~0%, 1% and 3%. We don't have any information on the accuracy of these values. Figure 5(a)-(c) shows the dark line pattern observed for each concentration, while Fig. 5(d) gives the refractive index, calibrated with the Pulfrich refractometer using water/ethanol solutions, and the attenuation coefficient, calibrated in transmission measurements of the 532 nm collimated laser beam through a 200 μm -thick quartz cell containing either our milk samples or the water/ethanol solution as reference [8]. In order for the transmission measurements to follow a straight line, we assumed that the concentration for the low fat sample was 0.2%. Note that the attenuation coefficients that we obtained are higher than those reported in the literature [2, 4] probably because we are using a shorter wavelength and the scattering is higher.

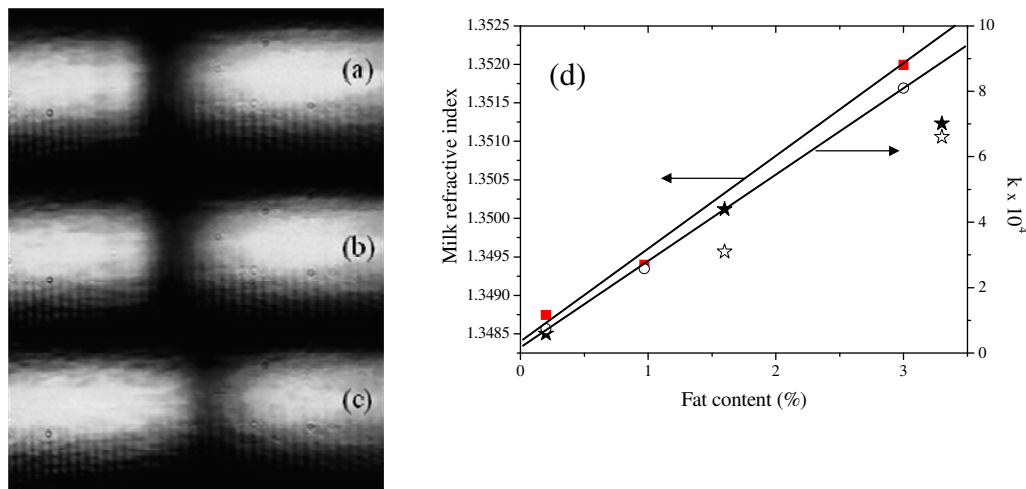


Fig. 5. Dark line pattern observed for fat concentrations of (a) 0%, (b) 1% and (c) 3%. (d) Dependence of the refractive index (solid squares) and attenuation coefficient (open circles) on the fat concentration. The refractive index was calibrated with the Pulfrich refractometer using water/ethanol solutions and the attenuation coefficient was calibrated through the transmission of a collimated beam through the samples. The solid (open) stars correspond to the refractive index (attenuation) obtained in [4]. The solid lines are just guides for the eye.

4. Conclusions

We presented a very simple method of determining the critical angle taking advantage of the different phases that *s*- and *p*-polarizations acquire upon internal reflection. The light reflected by the interface between the base of the semi-cylindrical lens and the sample presents a dark line that can be used to find the real (position of the line) and imaginary (value of the minimum) parts of the complex refractive index in real time. This method allowed the buildup of a sensitive, rugged and user friendly differential refractometer for transparent and turbid samples [10].

Acknowledgments:

We acknowledge the financial support from the Brazilian agencies: Fundação de Amparo à Pesquisa do Estado de São Paulo (FAPESP) and Conselho Nacional de Desenvolvimento Científico e Tecnológico (CNPq).